

ChemComm

Accepted Manuscript



This is an *Accepted Manuscript*, which has been through the Royal Society of Chemistry peer review process and has been accepted for publication.

Accepted Manuscripts are published online shortly after acceptance, before technical editing, formatting and proof reading. Using this free service, authors can make their results available to the community, in citable form, before we publish the edited article. We will replace this *Accepted Manuscript* with the edited and formatted *Advance Article* as soon as it is available.

You can find more information about *Accepted Manuscripts* in the [Information for Authors](#).

Please note that technical editing may introduce minor changes to the text and/or graphics, which may alter content. The journal's standard [Terms & Conditions](#) and the [Ethical guidelines](#) still apply. In no event shall the Royal Society of Chemistry be held responsible for any errors or omissions in this *Accepted Manuscript* or any consequences arising from the use of any information it contains.

COMMUNICATION

Pheomelanin-coated iron oxide magnetic nanoparticles: a promising candidate for negative T_2 contrast enhancement in magnetic resonance imaging

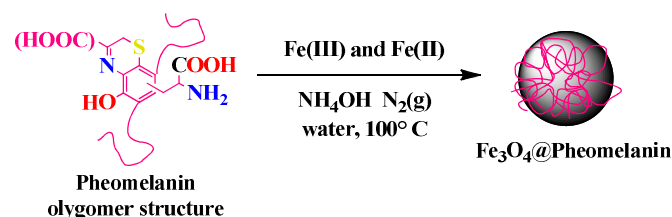
Cite this: DOI: 10.1039/x0xx00000x

Alexandre D. A Zottis^{a,b}, Jeovandro M. Beltrame^a, Luciano R. S. Lara^a, Thiago Costa^{a,c}, Mateus J. Feldhaus^a, Rozangela Curi Pedrosa^d, Fabiana Ourique^d, Carlos E. M. de Campos^e, Eduardo de A. Isoppo^e, Fabio da Silva Miranda^f and Bruno Szpoganicz^{*a}

We describe herein a novel type of monodisperse water-soluble magnetite nanoparticle coated with pheomelanin using an environmental-friendly approach in aqueous medium. The results indicate superparamagnetic behaviour at room temperature and show improved negative contrast in T_2 -weighted MRI with a transverse relaxivity of $218 \text{ mM}^{-1}\text{s}^{-1}$.

In recent decades there has been considerable interest in the preparation of iron oxide magnetic nanoparticles (IOMNPs) and a vast number of studies have been carried out involving biomedical applications.¹ Notable among these are nanocatalysis, biological separation, theranostics and, mainly, their use as contrast agents in magnetic resonance imaging (MRI).² In MRI, for biomedical applications the IOMNPs must be generally monodisperse, have a mean core size of up to 15 nm, are highly crystalline, allow high magnetization values and have good biocompatibility.³ For this proposal, a stabilizer is required, which must coat the IOMNPs and also serves to prevent the agglomeration of these ferrofluids.⁴ Recently, studies have been reported in which catechol-derived anchors, such as dopamine and their end groups, have been used to coat MNPs of Fe_3O_4 (10–20 nm), which are dispersible in water.⁵ Indeed, melanins exhibit interesting and unique properties including photo-protection, free-radical scavenging and antioxidant activity.⁶ In particular, pheomelanins are promising candidates for this coating since they contain an abundance of catechol groups, which can interact with and consequently stabilize the IOMNPs.⁷ However, until now, there have been no reports on studies involving the coating of IOMNPs using melanins, particularly pheomelanin (since it is soluble in water), as a negative T_2 contrast enhancement in MRI. In this communication, we report a novel type of water-soluble nanomaterial using pheomelanin as a coating material for MNPs of Fe_3O_4 , as outlined in Scheme 1. The synthesis of the pheomelanin-coated magnetite IOMNPs was carried out according to the co-precipitation approach with modifications.⁸ In brief, chloride salts of iron (II and III) in aqueous medium were

maintained in an acidic solution (1.0 M HCl) and the chemical reaction in the presence of alkali base and pheomelanin, at a temperature below 100°C , originated, as the final product, a dark brownish solution labelled $\text{Fe}_3\text{O}_4@\text{Pheo}$.



Scheme 1: Reaction scheme for the synthesis of iron oxide magnetic nanoparticles (IOMNPs) coated with pheomelanin.

The details of the synthetic procedures are provided in ESI†. The pheomelanin-coated magnetite IOMNPs showed relative monodispersity and high crystallinity with an average size of 10 nm, obtained by transmission electron microscopy (TEM-100 kV) and surface area electron diffraction (SAED) (Fig. 1A and 1B, respectively). The average crystalline domains and core size were around 13 nm, as estimated from the X-ray powder diffraction (XRPD) analysis results (Fig. 1C). The lattice parameter $a=8.3632 \text{ \AA}$ obtained via the Rietveld method applied to the XRPD data (0.2522 nm for (311)) is consistent with the value of 8.3181 \AA based on the (311) plane spacing of 0.2508 nm obtained employing SAED (Fig S1, ESI†). These results are also in agreement with the results of other studies related to the spinel-structure Fe_3O_4 and standard measurements ($a=8.3940$) (for further details, see Table S1, ESI†).⁹

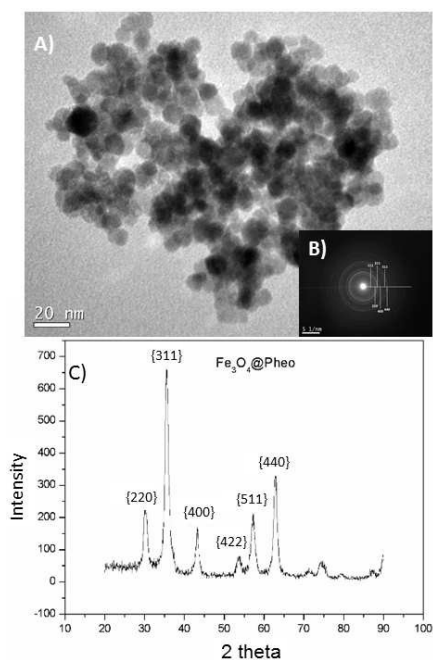


Fig. 1 (A) Low magnification TEM image of pheomelanin-coated iron oxide magnetic nanoparticles. (B) SAED of iron oxide nanoparticles. (C) XRPD diffractogram of iron oxide core coated with pheomelanin, with diffraction peaks indexed to spinel iron oxide phase.

The core size (below 15 nm) can also be estimated using VSM analysis, which indicates the super paramagnetic behaviour of the pheomelanin-coated magnetite IOMNPs, according to a previous publication.¹ Indeed, the nanoparticles exhibited low coercivity and a suitable saturation magnetization (M_s) value (52.5 emu.g^{-1}) at 300 K in comparison with other previously reported stabilizers obtained using this approach to the synthesis (for details see Fig. S2 and Table S2 of ESI[†]). The stabilization between the pheomelanin and the IOMNPs was also evident based on the FTIR spectra, indicated by the vibration frequencies at 1063 cm^{-1} (C-O stretching), associated with the phenolic ring, 1633 cm^{-1} (carboxylate or C=C ring as well as nitrogen containing heterocycles) and 590 cm^{-1} related to the Fe-O bond of Fe_3O_4 (for further details see Fig. S3, ESI[†]).¹⁰ The TGA curve allows the degree of pheomelanin coating (7.3% at around 500°C) onto the surface of the IOMNPs to be assessed. The literature suggests that this bio-oligomer demonstrates at least three different mass loss events between $280\text{--}500^\circ\text{C}$, which is associated with the indolequinone, benzothiazole and benzothiazine.¹¹ Lastly, the destabilization of melanin (at above 500°C) demonstrates that the mass loss was in agreement with reported values (6–62.5%) (see Fig. S4, ESI[†]).^{11c, 12} Indeed, the thermogravimetric and FT-IR data were consistent with the elemental analysis and EDX results (see Table S3 and S4, ESI[†]), respectively. Additionally, the X-ray photoelectron spectroscopy (XPS) analysis of the particles showed two further peaks at 710.2 and 724.9 eV, attributed to $\text{Fe}2p_{3/2}$ and $\text{Fe}2p_{1/2}$, (see Fig. S5, ESI[†]) respectively, which is related to the magnetite in agreement with the XRPD and the literature results.¹³ However, the presence of two smooth satellite peaks at 718.5 and 732.1 eV was noted (Fig. S6,

ESI[†]), suggesting that there is an oxidized phase ($\gamma\text{-Fe}_2\text{O}_3$) on the surface of the magnetite core. Furthermore, our results are in agreement with previously reported data that is, the O1s spectrum showed a peak with a binding energy close to 529 eV (Fig. S7, ESI[†]), which is assigned to the Fe-O binding in Fe_3O_4 .^{9b, 13a, 14} Furthermore, with respect to the carbon peak positions (C1s), a peak with a binding energy of 284.6 eV assigned to Fe-C was observed (Fig. S8, ESI[†]), this being the same value reported for a graphitic structure (aromatic ring), possibly due to the melanin structure.^{11b, 11c} Moreover, this corresponds to the organic surface coating, indicated by the aromatic rings, ranging between 286 and 288 eV (but less intense, since it represents only a broadening of the main peak) due to C-O and the binding energy of the phenol and carboxylate of pheomelanin, as observed for dopamine-coated IOMNPs and the corresponding to FTIR spectra (Fig. S3, ESI[†]) and literature.¹⁴ In order to assess the MRI signal enhancement effects, the aqueous solutions of as-prepared IOMNPs coated with pheomelanin at the different Fe concentrations (determined by flame absorption atomic spectroscopy (FAAS)) were kept on gel agar phantom to avoid aggregation of the ferrofluids. The relaxation rates were then measured on a clinical 1.5 T MRI scanner according to certain pulse sequences (further details in ESI[†]). It can be noted in Fig. 2A that the signal intensity of the T_2 -weighted images changed considerably increases with the iron concentration. The enhancement of the T_2 reduction effect (51.5, 57.3, 74.1 and 82.2%) in comparison to the control (agar gel solution) corresponding to 0.02, 0.04, 0.10 and 0.20 mM of [Fe], respectively can be observed in Fig. 2B.

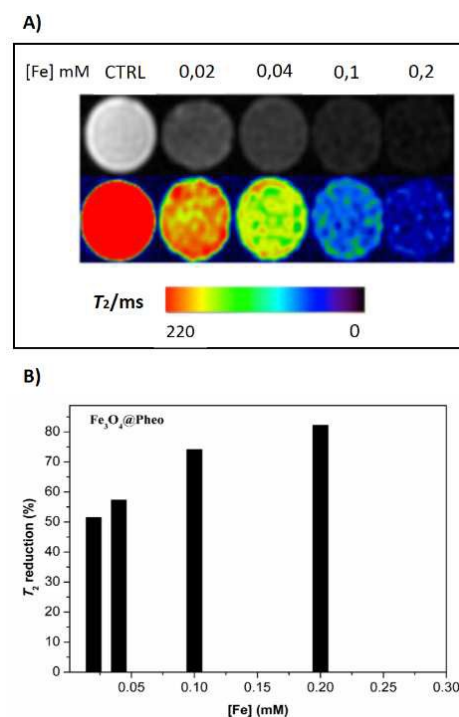


Fig.2 (A) T_2 -weighted MRI images - signal intensity versus iron concentration and (B) enhancement of T_2 reduction effect of pheomelanin-coated magnetic nanoparticles.

Furthermore, applying a given equation reported in the literature, a plot of the relaxation rates $1/T_1$ and $1/T_2$ as a function of the iron concentration (equation 2S and 4S, ESI[†]) could be obtained of (equation 1S ESI[†]) and also the relaxation T_2 curve (Fig. S9, ESI[†]).¹ Fig. 3A and 3B both show a linear dependency and the curve fitting provided good correlations ($R^2 = 0.9989$ for r_1 and 0.9473 for r_2 , respectively). Our results show a greater transverse relaxivity r_2 ($218 \text{ mM}^{-1}\text{s}^{-1}$) than longitudinal relaxivity r_1 ($1.6 \text{ mM}^{-1}\text{s}^{-1}$), where the negative T_2 contrast enhancement ($R_2 = 136$) for MRI is featured. Moreover, in this study the R_2 value was around 20 times higher than that reported for IOMNPs coated with chitosan, and also the r_2 value was three times higher than that obtained with chitosan as shown in Table 1.¹⁵

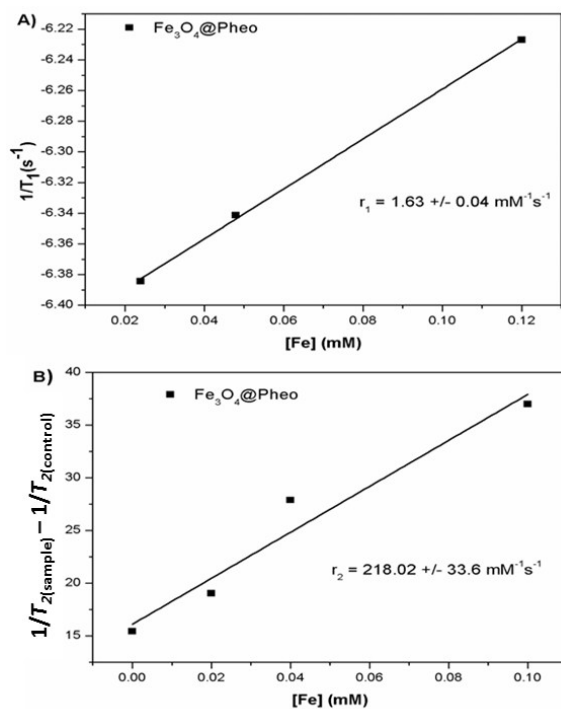


Fig. 3 (A) T_1 relaxation rates ($1/T_1$) and (B) T_2 ($_{sample} - T_2$ ($_{control}$)) relaxation rates plotted against the iron concentration for the magnetite nanoparticles in aqueous solution to obtain the longitudinal (r_1) and transverse relaxivities (r_2), respectively.

On the other hand, the r_2 values in this study were around three times higher compared with results for POA@IOMNPs (a copolymer PF127/oleic acid used as coating) with a hydrophobic surface, while the R_2 values were the same.¹⁶ This highlights that pheomelanin-coated magnetite IOMNPs could combine high-performance and hydrophilicity, verifying that they represent a promising candidate as a negative T_2 contrast enhancement for MRI (for further details see Fig. S9, ESI[†]). It is worth to notice that M_s (see ESI Table S2) has somewhat the same value in comparison to the other previously reported IOMNPs by using the similar approach to synthesize. Therefore, the enhancement of negative contrast performance is attributed to the pheomelanin coating. Moreover, in function of iron oxide core size and the coating (thickness and chemical composition) the T_2 shortening effect of IOMNPs could be estimated based of a quantum-mechanical outer-sphere theory.¹⁷ If being considered a simple manner, according to

equation (1), it could be noticed that transverse relaxivity T_2 decreases as the coating becomes thicker.

$$1/T_2 \propto 1 / (1 + L/a) \quad (1)$$

Where L is the thickness of coating material and a is the core size of IOMNPs. Comparing our pheomelanin coated IOMNPs with the chitosan coated ones (Table 1), the T_2 relaxivity is about twofold.

The dynamic light scattering (DLS) measurements (Fig. S10, ESI[†]) also indicated that the IOMNPs coated with pheomelanin could be kept dispersible in aqueous medium, after they had been stabilized in buffer solution (zeta potential ζ of -38.1mV) in $\text{pH} = 8.0$, (Fig. S11) close to physiological conditions. Furthermore, the hydrodynamic size of the IOMNPs was increased due to the presence of the hydrated pheomelanin layer. Thus, good monodispersivity was observed (see Fig. S10, ESI[†]). Since the pheomelanin-coated IOMNPs could be stabilized in aqueous solution, we employed as-synthesized IOMNPs to analyse the cytotoxicity toward MCF-7 cells using the MTT assay (for details see Fig. S12, ESI[†]). The results indicated 100% cell viability in the presence of pheomelanin-coated IOMNPs up to 0.2 mM $[\text{Fe}]$ and around 75% cell viability at the higher concentration of 0.4 mM $[\text{Fe}]$. Thus, it appears that pheomelanin-coated IOMNPs exhibit good biocompatibility and are safe for further *in vivo* and *in vitro* studies, which are already being carried out by our research group.

Table 1: Transverse relaxivities of iron oxide nanoparticles with different stabilizers measured at 1.5 T, at 20°C.

Stabilizers	diameter (nm)[c]	r_2 $\text{mM}^{-1}\text{s}^{-1}$	r_1 $\text{mM}^{-1}\text{s}^{-1}$	R_2 (r_2/r_1)	Ref.
Pheo	90	218.02	1.60	136	This work
CA ^[a]	150	155.7	3.5	44.5	18
PAA ^[a]	172	232.4	3.9	59.6	
Chitosan	130	64.31	9.44	6.8	15
Pluronic ^[b]	71	63.4	1.33	47.7	16
F127/OA					
Lactoferrin	75	75.6	-	-	19

[a] Citric Acid and Polyacrylic acid; [b] Copolymer F127 (measured at 37 °C) [c] Mean hydrodynamic size

In summary, we report a novel type of coating material comprised of a modified bio-oligomer containing a catechol group which interacts and stabilizes Fe_3O_4 nanoparticles. Thus, it was possible to produce these pheomelanin-coated IOMNPs using an environmentally-friendly and safer approach, since the use of organic solvents, the employment of time consuming steps in the synthesis and complex modification were not required. In addition, pheomelanin proved to be highly beneficial for biomedical applications. This approach opens up new opportunities for functionalization with biomolecules or any other terminal organic group (amide, amine, carboxylic, etc.). Therefore, it can be concluded that this novel class of IOMNPs has significant potential as a high-performance agent for negative T_2 contrast for breast cancer investigation using MRI as a non-invasive diagnosis tool.

This research was partially supported by the Brazilian National Research Council CNPq (452629/2014-4). B.S and A.D.Z are grateful to the Central Laboratory of Electron Microscopy (LCME) at UFSC (TEM analysis) as well as to Alexandre C.Viegas for the VSM measurements. On addition, special thanks are due to

Josiel B. Domingos from the Laboratory of Catalysis Biomimetics (LACBIO) at UFSC for the final revision of this manuscript, and Dr. Luiz F. Nobre for collaboration involving MRI analysis.

^a Academic Department of Health and Services, Nucleus of Clinical Technology, Instituto Federal de Educação, Ciência e Tecnologia de Santa Catarina, Campus Florianópolis, SC, 88020-300, Brazil. E-mail: adz@ifsc.edu.br; Tel: +55 4832210569

^b Chemistry Department, Universidade Federal de Santa Catarina, Trindade Campus, Florianópolis, SC, 88040-900, Brazil. E-mail: bruno.s@ufsc.br; Tel: +55 4837216847 Extension 216

^c Laboratório do Ateliê de Conservação e Restauração de Bens Culturais Móveis, Fundação Catarinense de Cultura, Florianópolis, SC, 88025-202, Brazil

^d Experimental Biochemistry Laboratory, Biochemistry Department, Universidade Federal de Santa Catarina, Trindade Campus, Florianópolis, SC, 88040-900, Brazil

^e Physics Department, Universidade Federal de Santa Catarina, Trindade Campus, Florianópolis, SC, 88040-900, Brazil

^f Instituto de Química, Universidade Federal Fluminense Outeiro de São João Batista, Niterói, RJ, 24020-141, Brazil

†Electronic Supplementary Information (ESI) available: Materials and methods for magnetic nanoparticle synthesis and supporting FT-IR, XPS spectra, size-distributions and relaxivity data. See DOI: 10.1039/c000000x/

Notes and references

- N. Lee and T. Hyeon, *Chemical Society Reviews*, 2012, **41**, 2575.
- (a) L. R. S. Lara, A. D. Zottis, W. C. Elias, D. Faggion, C. E. Maduro de Campos, J. J. S. Acuna and J. B. Domingos, *Rsc Adv*, 2015, **5**, 8289; (b) S. Shen, F. F. Kong, X. M. Guo, L. Wu, H. J. Shen, M. Xie, X. S. Wang, Y. Jin and Y. R. Ge, *Nanoscale*, 2013, **5**, 8056; (c) L. H. Shen, J. F. Bao, D. Wang, Y. X. Wang, Z. W. Chen, L. Ren, X. Zhou, X. B. Ke, M. Chen and A. Q. Yang, *Nanoscale*, 2013, **5**, 2133.
- J. Gallo, N. J. Long and E. O. Aboagy, *Chem Soc Rev*, 2013, **42**, 7816.
- S. Laurent, D. Forge, M. Port, A. Roch, C. Robic, L. Vander Elst and R. N. Muller, *Chemical Reviews*, 2008, **108**, 2064.
- A. K. Yuen, G. A. Hutton, A. F. Masters and T. Maschmeyer, *Dalton Trans*, 2012, **41**, 2545.
- (a) Y. Liu, L. Hong, K. Wakamatsu, S. Ito, B. Adhyaru, C.-Y. Cheng, C. R. Bowers and J. D. Simon, *Photochemistry and Photobiology*, 2005, **81**, 135; (b) A. D. Schweitzer, E. Revskaya, P. Chu, V. Pazo, M. Friedman, J. D. Nosanchuk, S. Cahill, S. Frases, A. Casadevall and E. Dadachova, *International journal of radiation oncology, biology, physics*, 2010, **78**, 1494; (c) R. C. Howell, A. D. Schweitzer, A. Casadevall and E. A. Dadachova, *Nuclear medicine and biology*, 2008, **35**, 353.
- (a) T. G. Costa, B. Szpoganicz, G. F. Caramori, V. R. De Almeida, A. S. Mangrich and A. P. Mangoni, *J Coord Chem*, 2014, **67**, 986; (b) T. G. Costa, R. Younger, C. Poe, P. J. Farmer and B. Szpoganicz, *Bioinorg Chem Appl*, 2012.
- A. Bee, R. Massart and S. Neveu, *Journal of Magnetism and Magnetic Materials*, 1995, **149**, 6.
- (a) R. Frison, G. Cernuto, A. Cervellino, O. Zaharko, G. M. Colonna, A. Guagliardi and N. Masciocchi, *Chem Mater*, 2013, **25**, 4820; (b) D. R. Lide, *CRC Handbook of Chemistry and Physics*, Taylor and Francis, Boca Raton, FL, 2007.
- (a) S. L. Easo and P. V. Mohanan, *Carbohydrate polymers*, 2013, **92**, 726; (b) B. Bilińska, *Spectrochimica Acta Part A: Molecular and Biomolecular Spectroscopy*, 2001, **57**, 2525.
- (a) A. M. Gómez-Marín and C. I. Sánchez, *Journal of Non-Crystalline Solids*, 2010, **356**, 1576; (b) S. N. Dezidério, C. A.

- Brunello, M. I. N. da Silva, M. A. Cotta and C. F. O. Graeff, *Journal of Non-Crystalline Solids*, 2004, **338-340**, 634; (c) C. Xin, J. H. Ma, C. J. Tan, Z. Yang, F. Ye, C. Long, S. Ye and D. B. Hou, *Journal of bioscience and bioengineering*, 2015, **119**, 446.
- B. Simonovic, V. Vucelic, A. Hadzi-Pavlovic, K. Stepien, T. Wilczok and D. Vucelic, *Journal of Thermal Analysis*, 1990, **36**, 2475.
- (a) Y. Tian, B. Yu, X. Li and K. Li, *Journal of Materials Chemistry*, 2011, **21**, 2476; (b) H. Gu, K. Xu, Z. Yang, C. K. Chang and B. Xu, *Chemical communications*, 2005, 4270.
- M. Zhang, X. He, L. Chen and Y. Zhang, *Journal of Materials Chemistry*, 2010, **20**, 10696.
- C. Sanjai, S. Kothan, P. Gonil, S. Saesoo and W. Sajomsang, *Carbohydrate polymers*, 2014, **104**, 231.
- J. Qin, S. Laurent, Y. S. Jo, A. Roch, M. Mikhaylova, Z. M. Bhujwalla, R. N. Muller and M. Muhammed, *Advanced Materials*, 2007, **19**, 1874.
- S. Tong, S. Hou, Z. Zheng, J. Zhou and G. Bao, *Nano Lett*, 2010, **10**, 4607.
- A. Jedlovsky-Hajdú, E. Tombácz, I. Bányai, M. Babos and A. Palkó, *Journal of Magnetism and Magnetic Materials*, 2012, **324**, 3173.
- H. Xie, Y. Zhu, W. Jiang, Q. Zhou, H. Yang, N. Gu, Y. Zhang, H. Xu, H. Xu and X. Yang, *Biomaterials*, 2011, **32**, 495.